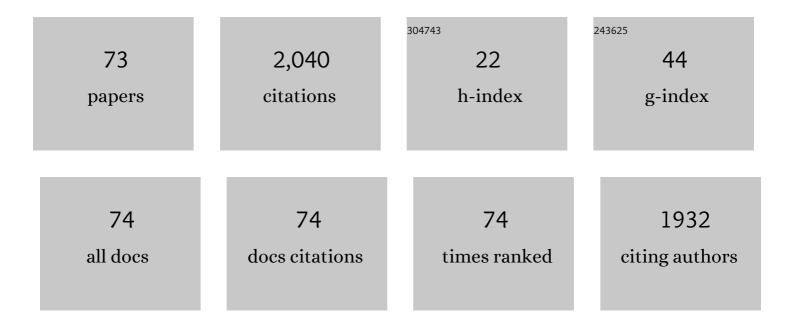
List of Publications by Year in descending order

Source: https://exaly.com/author-pdf/3266420/publications.pdf Version: 2024-02-01



#	Article	IF	CITATIONS
1	The geomorphology, color, and thermal properties of Ryugu: Implications for parent-body processes. Science, 2019, 364, 252.	12.6	313
2	Thermal and mechanical properties of the near-surface layers of comet 67P/Churyumov-Gerasimenko. Science, 2015, 349, aab0464.	12.6	158
3	A soft solid surface on Titan as revealed by the Huygens Surface Science Package. Nature, 2005, 438, 792-795.	27.8	139
4	Low thermal conductivity boulder with high porosity identified on C-type asteroid (162173) Ryugu. Nature Astronomy, 2019, 3, 971-976.	10.1	124
5	Boulder size and shape distributions on asteroid Ryugu. Icarus, 2019, 331, 179-191.	2.5	107
6	Highly porous nature of a primitive asteroid revealed by thermal imaging. Nature, 2020, 579, 518-522.	27.8	100
7	Mupus – A Thermal and Mechanical Properties Probe for the Rosetta Lander Philae. Space Science Reviews, 2007, 128, 339-362.	8.1	95
8	Thermal Infrared Imaging Experiments of C-Type Asteroid 162173 Ryugu on Hayabusa2. Space Science Reviews, 2017, 208, 255-286.	8.1	64
9	A Pre-Landing Assessment of Regolith Properties at the InSight Landing Site. Space Science Reviews, 2018, 214, 1.	8.1	58
10	Penetrators for in situ subsurface investigations of Europa. Advances in Space Research, 2011, 48, 725-742.	2.6	51
11	Particle lifting at the soil-air interface by atmospheric pressure excursions in dust devils. Geophysical Research Letters, 2006, 33, .	4.0	49
12	Fragment shapes in impact experiments ranging from cratering to catastrophic disruption. Icarus, 2016, 264, 316-330.	2.5	43
13	Recent Basal Melting of a Mid‣atitude Glacier on Mars. Journal of Geophysical Research E: Planets, 2017, 122, 2445-2468.	3.6	43
14	Asteroid Ryugu before the Hayabusa2 encounter. Progress in Earth and Planetary Science, 2018, 5, .	3.0	39
15	In situ methods for measuring thermal properties and heat flux on planetary bodies. Planetary and Space Science, 2011, 59, 639-660.	1.7	34
16	Anomalously porous boulders on (162173) Ryugu as primordial materials from its parent body. Nature Astronomy, 2021, 5, 766-774.	10.1	30
17	Descent motions of the Huygens probe as measured by the Surface Science Package (SSP): Turbulent evidence for a cloud layer. Planetary and Space Science, 2007, 55, 1936-1948.	1.7	29
18	Comet 67P/Churyumov–Gerasimenko: Hardening of the sub-surface layer. Icarus, 2015, 260, 464-474.	2.5	28

#	Article	IF	CITATIONS
19	Planetary heat flow measurements. Philosophical Transactions Series A, Mathematical, Physical, and Engineering Sciences, 2005, 363, 2777-2791.	3.4	25
20	Ejecta deposit thickness, heat flow, and a critical ambiguity on the Moon. Geophysical Research Letters, 2006, 33, .	4.0	24
21	A heat flow and physical properties package for the surface of Mercury. Planetary and Space Science, 2001, 49, 1571-1577.	1.7	23
22	Experimental investigation of insolation-driven dust ejection from Mars' CO2 ice caps. Icarus, 2017, 282, 118-126.	2.5	22
23	Boulder sizes and shapes on asteroids: A comparative study of Eros, Itokawa and Ryugu. Icarus, 2021, 357, 114282.	2.5	22
24	Penetrometry of granular and moist planetary surface materials: Application to the Huygens landing site on Titan. Icarus, 2010, 210, 843-851.	2.5	21
25	Clastic polygonal networks around Lyot crater, Mars: Possible formation mechanisms from morphometric analysis. Icarus, 2018, 302, 386-406.	2.5	21
26	Speed of sound measurements and the methane abundance in Titan's atmosphere. Icarus, 2007, 189, 538-543.	2.5	19
27	Physical properties of Titan's surface at the Huygens landing site from the Surface Science Package Acoustic Properties sensor (API-S). Icarus, 2006, 185, 457-465.	2.5	18
28	LunarEX—a proposal to cosmic vision. Experimental Astronomy, 2009, 23, 711-740.	3.7	18
29	Mapping Medusae Fossae Formation materials in the southern highlands of Mars. Icarus, 2010, 209, 405-415.	2.5	18
30	Sinuous ridges in Chukhung crater, Tempe Terra, Mars: Implications for fluvial, glacial, and glaciofluvial activity. Icarus, 2021, 357, 114131.	2.5	18
31	Prelaunch performance evaluation of the cometary experiment MUPUS-TP. Journal of Geophysical Research, 2004, 109, .	3.3	17
32	Influence of petrographic textures on the shapes of impact experiment fine fragments measuring several tens of microns: Comparison with Itokawa regolith particles. Icarus, 2018, 302, 109-125.	2.5	17
33	Lunar Net—a proposal in response to an ESA M3 call in 2010 for a medium sized mission. Experimental Astronomy, 2012, 33, 587-644.	3.7	15
34	Near Surface Properties of Martian Regolith Derived From InSight HP <sup>3</sup> â€RAD Temperature Observations During Phobos Transits. Geophysical Research Letters, 2021, 48, e2021GL093542.	4.0	13
35	Silence on Shangri-La: Attenuation of Huygens acoustic signals suggests surface volatiles. Planetary and Space Science, 2014, 90, 72-80.	1.7	12
36	Clastic patterned ground in Lomonosov crater, Mars: examining fracture controlled formation mechanisms. Icarus, 2017, 295, 125-139.	2.5	12

#	Article	IF	CITATIONS
37	Constraining the parameter space of comet simulation experiments. Icarus, 2018, 311, 105-112.	2.5	12
38	CO <sub>2</sub> sublimation in Martian gullies: laboratory experiments at varied slope angle and regolith grain sizes. Geological Society Special Publication, 2019, 467, 343-371.	1.3	12
39	Morphometry of a glacier-linked esker in NW Tempe Terra, Mars, and implications for sediment-discharge dynamics of subglacial drainage. Earth and Planetary Science Letters, 2020, 542, 116325.	4.4	12
40	A method to invert MUPUS. Temperature recordings for the subsurface temperature field of P/Wirtanen. Advances in Space Research, 1999, 23, 1333-1336.	2.6	11
41	A branching, positive relief network in the middle member of the Medusae Fossae Formation, equatorial Mars—Evidence for sapping?. Planetary and Space Science, 2013, 85, 142-163.	1.7	11
42	Oblique impact cratering experiments in brittle targets: Implications for elliptical craters on the Moon. Planetary and Space Science, 2017, 135, 27-36.	1.7	11
43	The Penetration of Solar Radiation Into Carbon Dioxide Ice. Journal of Geophysical Research E: Planets, 2018, 123, 864-871.	3.6	11
44	Earth and moon observations by thermal infrared imager on Hayabusa2 and the application to detectability of asteroid 162173 Ryugu. Planetary and Space Science, 2018, 158, 46-52.	1.7	10
45	Hardness and Yield Strength of CO Ice Under Martian Temperature Conditions. Journal of Geophysical Research E: Planets, 2020, 125, e2019JE006217.	3.6	10
46	Thermal and microstructural properties of fine-grained material at the Viking Lander 1 site. Icarus, 2016, 271, 360-374.	2.5	9
47	Computer modelling of a penetrator thermal sensor. Advances in Space Research, 2010, 46, 337-345.	2.6	8
48	Penetration of solar radiation into pure and Mars-dust contaminated snow. Icarus, 2015, 252, 144-149.	2.5	8
49	In situ thermal conductivity measurements of Titan's lower atmosphere. Icarus, 2008, 197, 579-584.	2.5	7
50	Virial treatment of the speed of sound in cold, dense atmospheres and application to Titan. Monthly Notices of the Royal Astronomical Society, 2006, 368, 321-324.	4.4	6
51	The Penetration of Solar Radiation Into Granular Carbon Dioxide and Water Ices of Varying Grain Sizes on Mars. Journal of Geophysical Research E: Planets, 2020, 125, e2019JE006097.	3.6	6
52	Physical properties as indicators of liquid compositions: Derivation of the composition for Titan's surface liquids from the Huygens SSP measurements. Monthly Notices of the Royal Astronomical Society, 2005, 359, 637-642.	4.4	5
53	Impact cratering experiments in brittle targets with variable thickness: Implications for deep pit craters on Mars. Planetary and Space Science, 2014, 96, 71-80.	1.7	5
54	Detection of structure in asteroid analogue materials and Titan's regolith by a landing spacecraft. Advances in Space Research, 2016, 58, 415-437.	2.6	5

#	Article	IF	CITATIONS
55	Three-dimensional imaging of crack growth in L chondrites after high-velocity impact experiments. Planetary and Space Science, 2019, 177, 104690.	1.7	5
56	The Penetration of Solar Radiation Into Water and Carbon Dioxide Snow, With Reference to Mars. Journal of Geophysical Research E: Planets, 2019, 124, 337-348.	3.6	5
57	Thermal conductivity instrument for measuring planetary atmospheric properties and data analysis technique. Journal of Thermal Analysis and Calorimetry, 2007, 87, 585-590.	3.6	4
58	The Huygens scientific data archive: Technical overview. Planetary and Space Science, 2008, 56, 770-777.	1.7	4
59	The distribution of putative periglacial landforms on the martian northern plains. Icarus, 2018, 314, 133-148.	2.5	4
60	APPLICATION OF PENETRATORS WITHIN THE SOLAR SYSTEM. , 0, , 307-320.		4
61	Planetary heat flow from shallow subsurface measurements: Mars. Planetary and Space Science, 2016, 131, 46-59.	1.7	3
62	Gas flow in martian spider formation. Icarus, 2021, 359, 114355.	2.5	3
63	The modified Rankine balance: A highly efficient, low-cost method to measure low-temperature magnetic susceptibility in rock samples. Review of Scientific Instruments, 2002, 73, 2655-2658.	1.3	2
64	Speed of sound in nitrogen as a function of temperature and pressure. Journal of the Acoustical Society of America, 2005, 118, 1272-1273.	1.1	2
65	Inferring the composition of the liquid surface on Titan at the Huygens probe landing site from Surface Science Package measurements. Advances in Space Research, 2006, 38, 794-798.	2.6	2
66	Rosetta Lander ("Philaeâ€ <del>)</del> Investigations. , 2009, , 1-171.		2
67	Three-axial shape distributions of pebbles, cobbles and boulders smaller than a few meters on asteroid Ryugu. Icarus, 2022, 381, 115007.	2.5	1
68	A Simple Way of Simulating Insolation on a Rotating Body with a Commercial Solar Simulator. International Journal of Thermophysics, 2022, 43, .	2.1	1
69	Towards a Holistic Framework for Driving Performance in Externally-Funded Academic Research. Higher Education Quarterly, 2009, 63, 196-206.	2.7	0
70	UK Mars research and priorities in the Aurora programme. Astronomy and Geophysics, 2011, 52, 2.34-2.36.	0.2	0
71	WatSen: design and testing of a prototype mid-IR spectrometer and microscope package for Mars exploration. Experimental Astronomy, 2013, 36, 175-193.	3.7	0
72	Potential effects of atmospheric collapse on Martian heat flow and application to the InSight measurements. Planetary and Space Science, 2020, 180, 104778.	1.7	0

#	Article	IF	CITATIONS
73	Thermal Infrared Imaging Experiments of C-Type Asteroid 162173 Ryugu on Hayabusa2. , 2016, , 255-286.		Ο